Analyst

Accepted Manuscript

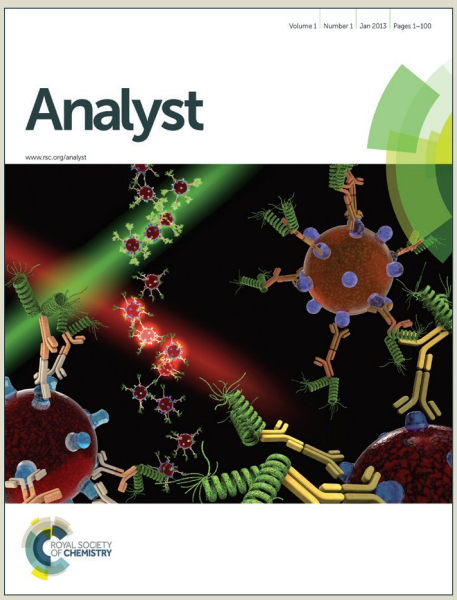

ROYAL SOCIETY OF CHEMISTRY

www.rsc.org/analyst

Analyst

RSCPublishing

ARTICLE

Superposition of an AC Field improves the discrimination between peptides in nanopore analysis.

Cite this: DOI: 10.1039/x0xx00000x

Elisabet Jakova, Jeremy S. Lee*

Received 00th January 2012,
Accepted 00th January 2012

DOI: 10.1039/x0xx00000x

www.rsc.org/

In standard nanopore analysis a constant DC voltage is used to electrophoretically drive small molecules and peptides towards a pore. Superposition of an AC voltage at particular frequencies causes molecules to oscillate as they approach the pore which can alter the event parameters, the blockade current (I) and blockade time (T). Four peptides with similar structures were studied. Alpha-helical peptides A10 ($FmocDDA_{10}KK$), A14, A18 and retro-inverso A10. It was shown that the ratio of translocations to bumping events could be manipulated by a combination of AC voltages and frequencies. In particular, A10 could be studied without interference from retro-inverso A10. Similarly, a large, intrinsically disordered protein of 140 amino acids, α-synuclein, which translocates the pore readily in a DC field could be prevented from doing so by application of an AC field of 200 mV at 100 MHz.

Introduction

The use of nanopores as an analytical tool dates back nearly twenty years.[1] The principle is similar to the Coulter Counter and relies on measuring a resistive pulse which occurs as an analyte passes through a small pore.[2-3] For small molecules, the blockade current (I) is of the order of pA which can be determined with a patch clamp apparatus. The initial results suggested that nanopores might allow rapid and efficient sequencing of nucleic acids but that goal has yet to be realized.[4-6] One particular advantage of nanopore analysis is that it can be performed at low concentrations with unlabelled analytes and thus it has found many applications in other areas. These include small molecule detection,[7] peptides and proteins,[8-10] protein folding,[11-14] and complex formation between metal ions/receptors,[15-17] peptide/drugs,[18] nucleic acid aptamers/drugs,[19-22] and even proteins/antibodies.[23] Most of this work has utilized the α-hemolysin pore because it readily self-assembles in a lipid bilayer giving a pore with reproducible dimensions and surface properties.[24] An interesting refinement has been to alter the amino acids in the lumen of the pore by protein engineering.[25] For example, the M113F mutation provides a more hydrophobic pore which enhances the denaturation of short DNA duplexes.[26] Solid state pores elaborated in silicon nitride membranes, for example, have also been studied but it is difficult to control the process and there is considerable batch to batch variation.[14, 27]

One problem with the α-hemolysin pore is that it is difficult to distinguish between molecules of a similar size since the blockade current (I) is determined by the occluded volume in the lumen as the molecule translocates and the characteristic time of the events (T) is difficult to estimate accurately especially for small molecules.[28] Several techniques have been developed to improve the discrimination between related molecules. These include addition of viscous solvents to increase the value of T, and covalent attachment of aptamers to the mouth of the pore to filter out unwanted analytes.[17, 29-30] As well, an AC field of 1-2 KHz has been used to measure current blockades in the absence of a DC field.[31]

When a peptide interacts with the pore there are usually two outcomes. Either it translocates through the pore giving a large current blockade or it bumps into the outside of the pore and then diffuses away giving a small current blockade. Under some conditions, a molecule may enter the vestibule of the pore without translocating. This type of event, termed intercalation, tends to give an intermediate current blockade (Fig. 1).[8, 32]

Previously, we demonstrated that superposition of an AC voltage at various frequencies in the MHz range on the electrophoretic DC voltage could modulate the translocation of small peptides through the α-hemolysin pore.[33] It was proposed that the AC voltage caused the peptides to rotate or oscillate dependent upon the dipole moment of the peptide. At an appropriate frequency, the molecular rotation would cause the peptide to bump into the pore rather than translocate (Fig.1). In support of this theory, peptides with no dipole moment were not affected by the addition of an AC field.[33]

In this paper, four α-helical peptides with similar structures were studied, namely A10, A14, A18 and retro-inverso A10. (Table 1)

It was shown that the ratio of translocations to bumping events could be manipulated by a combination of AC voltages and frequencies. The RI-A10 which has a large dipole moment (Table 1) could be prevented from translocating by applying an AC voltage of 200 mV at a frequency of 10 MHz. In particular, a mixture of A10, and RI-A10 could be analysed simultaneously. Similarly, a large, intrinsically disordered protein of 140 amino acids, α-synuclein (AS), which translocates the pore readily in a DC field could be largely prevented from doing so by application of an AC field of 200 mV at 100 MHz.

Experimental

A Peptides.

Peptides were acquired from CHI Scientific (Maynard, MA, USA) and dissolved in nanopore buffer (1 M KCl in 10 mM Phosphate buffer , pH 7.8) at a concentration of 2 mg/ml. The final concentration for analysis was 0.02 mg/ml. α-synuclein was purchased from rPeptides (Bogart, GA, USA) and used in a buffer of 10 mM HEPES, pH 8.0 and 1 M KCl at a final concentration of 1 μM.

B Nanopore analysis.

Instrument setup.

The standard DC setup has been described in detail previously.[20-22] Briefly, a lipid bilayer was painted onto a 150 μm aperture in a teflon perfusion cup which separated two buffer compartments of volume 1 mL. 5 μL of 1 μg/ml of α–hemolysin (Sigma-Aldrich, Canada) was added to the *cis* side of the membrane and the current was monitored until stable pore insertion was achieved. Consistent results were achieved with one to four pores. The peptides were added to the *cis*-side of the pore with the positive electrode on the *trans*-side. The experiments were carried out at 22 ± 1°C with an applied potential of 60 mV, 100 mV or 140 mV at a band width of 10 KHz using an Axopatch 200B amplifier (Axon Instruments) under voltage clamp conditions and Clampfit software. The AC voltage was applied directly to the two electrodes with an Agilent E4420B signal generator. The peak to peak voltage was constant at 200 mV and the frequency was varied between 10 MHz and 1 GHz. Frequencies in the KHz range would be picked up by the event recorder and experimentally little change in event profiles were observed above 500 MHz. As discussed elsewhere, temperature changes due to Joule heating are expected to be negligible.[34]

Data analysis.

The blockade amplitudes and duration times obtained with Clampfit were transferred to Origin 7 graphing software (OriginLab Corporation) and were used to construct blockade current and time histograms. The blockade amplitudes were plotted as statistical histograms and each event population (eg. translocation, intercalation and bumping) were fitted with a Gaussian function to obtain the peak/population blockade current value (I). The duration time data for each population was plotted separately and the data fitted with a single exponential decay function to obtain the characteristic time (T).

Results and discussion

Typical current traces covering a time period of about 6 s for A10 and RI-A10 with and without an AC voltage are shown in Fig. 2. (Expanded views of the event profiles are shown in Supplementary Figs 1-3). Each event is a spike with the longest spikes at about -70 pA due to translocations and the shorter spikes below -30 pA due to bumping events. Even in the absence of an AC field, the frequency of events for RI-A10 is lower than that for A10. As discussed previously, it is thought that the presence of the polarisable Fmoc group helps to steer the peptide into the pore.[8-9]

However, for RI-A10, the negative charge is at the C-terminus which will enter the pore first so that the Fmoc is now to the rear of the peptide.[35] As well, at this DC voltage of 100 mV the AC field has only a small effect on the A10 peptide in whereas a DC voltage of 60 mV, previously reported,[33] caused a large increase in the number of bumping events. In contrast for RI-A10 the number of translocation events is clearly reduced.

Current traces such as those of Fig. 2 were converted into blockade current histograms which allows a more detailed analysis of the event profiles. These are shown in Fig. 3 for A10 and Fig. 4 for RI-A10. For A10, there are three consequences of the application of an AC field. First, the translocation peak shifts from -63 pA to about -54 pA. The origin of this effect is not clear but it is not due to a change in the conformation of the α-hemolysin pore since the open pore current remains at -100 pA. One possibility is that the AC field allows the K^+ and Cl^- ions to move around the peptide more easily. Second, the AC field decreases the proportion of translocation events at all frequencies but this effect is only modest compared to that previously reported for 60 mV.[33] For example the % translocations at a frequency of 100 MHz were 54% at 60 mV but 71% at 100 mV. It seems likely that as the DC voltage increases, the AC field has less effect on the oscillation of the peptide as it approaches the entrance to the pore. Third, at higher frequencies, an intermediate peak appears at about -33 pA which is attributed to intercalation events. It seems possible that as the molecule enters the vestibule of the pore the AC field causes it to rotate so that it is perpendicular to the lumen of the pore and cannot make further progress (Fig. 1). When the AC field reverses, it will rotate in the opposite direction and then be ejected from the pore.

For RI-A10, the blockade current histograms are much simpler (Fig 4); at all AC frequencies the proportion of translocation events is reduced to < 5%. The simplest explanation, is that the larger dipole moment and/or the C-terminal negative charge compared to A10 allow easy access to the vestibule of the pore but not the lumen.

A10, A14 and A18 were analyzed at three different DC voltages but for simplicity only the blockade current histograms for A18 at 100 mV will be described in detail (Fig. 5). With no AC field there is a single Gaussian peak at -66 pA but with an AC field at a frequency of 10 MHz a second peak appears at -45 pA due to intercalation. On increasing the frequency to 100 MHz or higher a third bumping peak can be seen at -27 pA. There is also a shoulder at about -65 pA on the translocation peak which has become very sharp. Three peaks were also observed for A14 at 100 mV DC (data not shown). In contrast to A10 (Fig. 3) where the blockade current decreases with an AC field for A18 the blockade current increases to -73 pA. Curiously, for A18 at 140 mV DC the current blockade of the translocation events decreases on addition of an AC field (data not shown).

In order to provide a better understanding of the changes in the blockade currents, the characteristic times (T) for each of the Gaussian peaks were also measured. As an example, time histograms for A18 at 60 mV, 100 Mv and 140 mV at 50 MHz are shown in Fig.6. The fit to a single exponential is reasonable at each voltage but it is clear that the time at 100 mV is significantly longer. The results are summarized in Fig. 7. For all three peptides in the absence of an AC field, the time for translocation decreases with voltage and increases with the length of the peptide, as expected. In all cases the bumping or intercalation events are much faster. Addition of an AC field

does little to change this pattern for A10 and A14 but for A18 at both 50 and 500 MHz the time of the events reaches a maximum at 100 mV. In the absence of an AC field the value of T at 100 mV is about 0.40 ms but at 50 and 500 MHZ it is 1.55 ms and 1.25 ms respectively. As well, at 60 mV in the absence of an AC field T is 0.55 ms but at a frequency of 50 MHz it decreases to 0.28 ms. Thus an AC field at 50 MHz can dramatically decrease or increase the event times depending on the DC voltage. Thus the anomalous blockade current of A18 at 50 MHz and 100 mV DC (Fig. 5c) is also mirrored in an anomalous blockade time for these events (Fig. 6b and 7h).

Returning to Fig. 5c, we propose that the small shoulder at about -65 pA observed at frequencies of 50 MHz and above is due to translocation of A18 in a linear conformation as would be observed in the absence of an AC field. Consistent with this proposal is that the time of these events is 0.2 ms (data not shown). In contrast, the sharp peak at -73 pA is due to a bent conformation; the peptide begins to enter the lumen of the pore but the AC field is sufficient to break the α-helix so that part of the molecule remains in the vestibule. At some point, the peptide will reorient and continue to translocate but the blockade current will be slightly larger and the overall time for the event will be increased considerably. This putative bent conformation does not occur at 140 mV nor for A10 or A14 because these peptides are shorter and have a small dipole moment. This could be the reason why the AC field is insufficient to cause a conformational change.

AS is a peptide of 140 amino acids which is intrinsically disordered under most conditions.[36-37] It can misfold and form β-sheet containing aggregates which are thought to play a central role in Parkinson's Disease.[38-42] The C-terminus has a net charge of -12 whilst the N-terminus has a net charge of +4 and, therefore, it is electrophoretically driven through the pore from the C-terminus under standard conditions. Most random conformations of AS are expected to have a very large dipole moment and thus it was of interest to analyze the effect of an added AC field. As shown in Fig. 8, in the absence of an AC field the majority of events are translocations as observed previously.[42,43] However, as the frequency of the AC field increases so does the proportion of bumping events until at 1 GHz about 73% of the events are bumping. Thus, nanopore analysis with an AC field may be useful for probing the conformational states of AS which are induced by drugs or metal ions.[18-19]

Finally, this technique may also be applied to the discrimination of molecular mixtures. As an example, A10 and RI-A10 have very similar molecular properties even to the extent that antibodies raised against RI-A10 will bind to A10 and their individual blockade current profiles overlap (Fig. 3 and 4).[33,35] An equimolar mixture of the two peptides were analyzed without an AC field which gives rise to a broad translocation peak at -59 pA and a minor bumping peak (Fig. 9a). The calculated blockade current histogram also gives a broad translocation peak at 60 pA but the bumping peak is much smaller (Fig. 9d). Thus there may be a small degree of interference between the two peptides which causes a higher proportion of bumping events. Addition of an AC field at either 10 MHz or 100 MHz increases the proportion of bumping events as expected since the translocation of RI-A10 is prevented (Fig. 9b and c). There is also a good fit with the calculated blockade current histograms (Fig. 9e and f) especially at 100 MHz. Thus, addition of an AC field allows the analysis of A10 even in the presence of a related peptide.

Conclusions

The superposition of an AC field on a constant DC voltage during nanopore analysis can cause large changes to the event profiles. These changes include increases to the proportion of bumping events, the appearance of intercalation events and changes to the time of translocation events. The effect is due to interaction between the AC field and the dipole of the molecule and thus molecules with different dipole moments can be individually manipulated by appropriate adjustments to the DC voltage and AC frequency. In other words, the molecules can be made to dance to an electronic tune. It can also be applied to large peptides. This technique may find applications where increased discrimination is required between mixtures of related molecules or to study the many conformational states of intrinsically disordered proteins.

Acknowledgements

This work was funded by the National Science and Engineering Research Council of Canada by a discovery grant to JSL.

Notes and references

*Department of Biochemistry, 107, Wiggins Road, University of Saskatchewan, Saskatoon, SK, Canada S7N 0W0

1. J. J. Kasianowicz, E. Brandin, D. Branton and D. W. Deamer, *Proc. Natl. Acad. Sci. USA*, 1996, **93**, 13770-13773.
2. H. Bayley and C. R. Martin, *Chem. Rev.*, 2000, **100**, 2575-2594.
3. S. Howorka and Z. Siwy, *Chem. Soc. Rev*, 2009, **38**, 2360-2384.
4. J. Clarke, H.-C. Wu, L. Jayasinghe, A. Patel, S. Reid and H. Bayley, *Nat. Nanotechnol.*, 2009, **4**, 265-270.
5. G. F. Schneider and C. Dekker, *Nat. Biotechnol.*, 2012, **30**, 326-328.
6. G. M. Cherf, K. R. Lieberman, H. Rashid, C. E. Lam, K. Karplus and M. Akeson, *Nat. Biotech.*, 2012, **30**, 344-348.
7. A. J. Boersma and H. Bayley, *Angewandte Chemie*, 2012, **124**, 9744-9747.
8. C. Christensen, C. Baran, B. Krasniqi, R. I. Stefureac, S. Nokhrin and J. S. Lee, *J. Pept. Sci.*, 2011, **17**, 726-734.
9. R. Stefureac, Y.-t. Long, H.-B. Kraatz, P. Howard and J. S. Lee, *Biochemistry*, 2006, **45**, 9172-9179.
10. M. Mohammad and L. Movileanu, *Eur. Biophys. J.*, 2008, **37**, 913-925.
11. F. Chiti and C. M. Dobson, *Annu. Rev. Biochem.*, 2006, **75**, 333-366.
12. C. A. Madampage, O. Tavassoly, C. Christensen, M. Kumari and J. S. Lee, *Prion*, 2012, **6**, 116-123.
13. D. Rodriguez-Larrea and H. Bayley, *Nat. Nano.*, 2013, **8**, 288-295.
14. A. Oukhaled, B. Cressiot, L. Bacri, M. Pastoriza-Gallego, J.-M. Betton, E. Bourhis, R. Jede, J. Gierak, L. Auvray and J. Pelta, *ACS Nano.*, 2011, **5**, 3628-3638.
15. R. I. Stefureac, C. A. Madampage, O. Andrievskaia and J. S. Lee, *Biochem. Cell Biol.*, 2010, **88**, 347-358.
16. A. Asandei, I. Schiopu, S. Iftemi, L. Mereuta and T. Luchian, *Langmuir*, 2013, **29**, 15634-15642.

17. G. Wang, L. Wang, Y. Han, S. Zhou and X. Guan, *Biosens. Bioelectron.*, 2014, **53**, 453-458.
18. O. Tavassoly and J. S. Lee, *FEBS Lett.*, 2012, **586**, 3222-3228.
19. J. W. Shim, Q. Tan and L.-Q. Gu, *Nucl. Acids Res.*, 2009, **37**, 972-982.
20. B. M. Venkatesan and R. Bashir, *Nat. Nano.*, 2011, **6**, 615-624.
21. D. Rotem, L. Jayasinghe, M. Salichou and H. Bayley, *J. Am. Chem. Soc.*, 2012, **134**, 2781-2787.
22. J. Larkin, S. Carson, D. H. Stoloff and M. Wanunu, *Isr. J. Chem.*, 2013, **53**, 431-441.
23. C. A. Madampage, O. Andrievskaia and J. S. Lee, *Anal. Biochem.*, 2010, **396**, 36-41.
24. N. Jetha, M. Wiggin and A. Marziali, in *Micro and Nano Technologies in Bioanalysis*, eds. R. S. Foote and J. W. Lee, Humana Press, Editon edn., 2009, vol. 544, pp. 113-127.
25. L.-Q. Gu and H. Bayley, *Biophys. J.*, 2000, **79**, 1967-1975.
26. L.-Q. Gu, S. Cheley and H. Bayley, *J. Gen. Physiol.*, 2001, **118**, 481-494.
27. A. Janshoff and C. Steinem, *Anal. Bioanal. Chem.*, 2006, **385**, 433-451.
28. J. N. Jonathan, A. Mark and M. Andre, *J. Phys.: Condens. Matter*, 2003, **15**, R1365.
29. X. Guan, L.-Q. Gu, S. Cheley, O. Braha and H. Bayley, *Chem. Bio. Chem.*, 2005, **6**, 1875-1881.
30. D. A. Jayawardhana, J. A. Crank, Q. Zhao, D. W. Armstrong and X. Guan, *Anal. Chem.*, 2008, **81**, 460-464.
31. E. A. Ervin, R. Kawano, R. J. White and H. S. White, *Anal. Chem.,*2008, **80**, 2069-2076.
32. H. Meng, D. Detillieux, C. Baran, B. Krasniqi, C. Christensen, C. Madampage, R. I. Stefureac and J. S. Lee, *J. Pept. Sci.*, 2010, **16**, 701-708.
33. R. I. Stefureac, A. Kachayev and J. S. Lee, *Chem. Comm.*, 2012, **48**, 1928-1930.
34. F. Harb and B. Tinland, *Electrophoresis,* 2013, **34,** 3054-3063.
35. B. Krasniqi, E. Scruten, J. Piller, J. Lee and S. Napper, *J. Pept. Sci.*, 2012, **18**, 519-526.
36. M. Goedert, *Nat. Rev. Neurosci.*, 2001, **2**, 492-501.
37. A. Singleton, M. Farrer, J. Johnson, A. Singleton, S. Hague, J. Kachergus, M. Hulihan, T. Peuralinna, A. Dutra and R. Nussbaum, *Science*, 2003, **302**, 841-841.
38. A. L. Fink, *Accounts Chem. Res.*, 2006, **39**, 628-634.
39. S. C. Maria, S. Rabia, G. Erik, D. F. Gerardo, R. Jean-Marie and R. Vincent, *Biochem. J.*, 2012, **443**, 719-726.
40. A. Recchia, P. Debetto, A. Negro, D. Guidolin, S. D. Skaper and P. Giusti, *FASEB J.*, 2004, **18**, 617-626.
41. B. Shivu, S. Seshadri, J. Li, K. A. Oberg, V. N. Uversky and A. L. Fink, *Biochemistry*, 2013, **52**, 5176-5183.
42. O. Tavassoly, S. Nokhrin, O. Y. Dmitriev and J. S. Lee, *FEBS J.*, 2014, **281**, 2738-2753.
43. O. Tavassoly, J. Kakish, S. Nokhrin, O. Dmitriev and J. S. Lee, *Eur. J. Med. Chem.*, 2014, **88**, 42-54.

Table 1. The α-helical peptides.[8-9] RI-A10 has all D-amino acids.[35] The lengths and dipole moments were calculated with Spartan software.

Peptide	Length (Å)	Dipole moment (Debye)
Fmoc-DDA$_{10}$KK (A10)	28.2	260
Fmoc-DDA$_{14}$KK (A14)	33.7	329
Fmoc-DDA$_{18}$KK (A18)	39.1	400
Fmoc-KKA$_{10}$DD (RI-A10)	28.3	373

Figure Legends

Fig. 1. There are three possible types of events when a peptide interacts with the α-hemolysin pore. The AC field causes peptides to oscillate at the entrance of the pore.
Fig. 2. Current traces for A10 and RI-A10 with and without an AC field at a DC current of 100 mV.
Fig. 3. Blockade current histograms for A10 at 100 mV DC with a. No AC, b. 10 MHz, c. 50 MHz, d. 100 MHz, e. 500 MHz and f. 1 GHz AC.
Fig. 4. Blockade current histograms for RI-A10 at 100 mV DC with a. No AC, b. 10 MHz, c. 50 MHz, d. 100 MHz, e. 500 MHz and f. 1 GHz AC.
Fig. 5. Blockade current histograms for A18 at 100 mV DC with **a.** No AC, **b.** 10 MHz, **c.** 50 MHz, **d.** 100 MHz, **e.** 500 MHz and **f.** 1 GHz AC.
Fig. 6. Time histograms of translocation events for A18 at 50 MHz AC and DC voltages of 60, 100 and 140 mV.
Fig. 7. Event times as a function of the DC voltage for: **a.** A10, **d.** A14 and **g.** A18 with no AC frequency applied; **b.** A10, **e**. A14 and **h.** A18 with 50 MHz AC; and **c.** A10, **f.** A14 and **i.** A18 with 500 MHz AC.
Fig. 8. Blockade current histograms for AS at 100 mV DC with **a.** No AC, **b.** 10 MHz, **c.** 50 MHz, **d.** 100 MHz, **e.** 500 MHz and **f.** 1 GHz AC.
Fig. 9. Blockade current histograms for a mixture of A10 and RI-A10 at 100 mV DC for no AC, 10 MHz and 100 MHz applied. **a.**, **b.** and **c.** are values from the experiment; **d.**, **e.** and **f.** were calculated by adding the individual histograms.

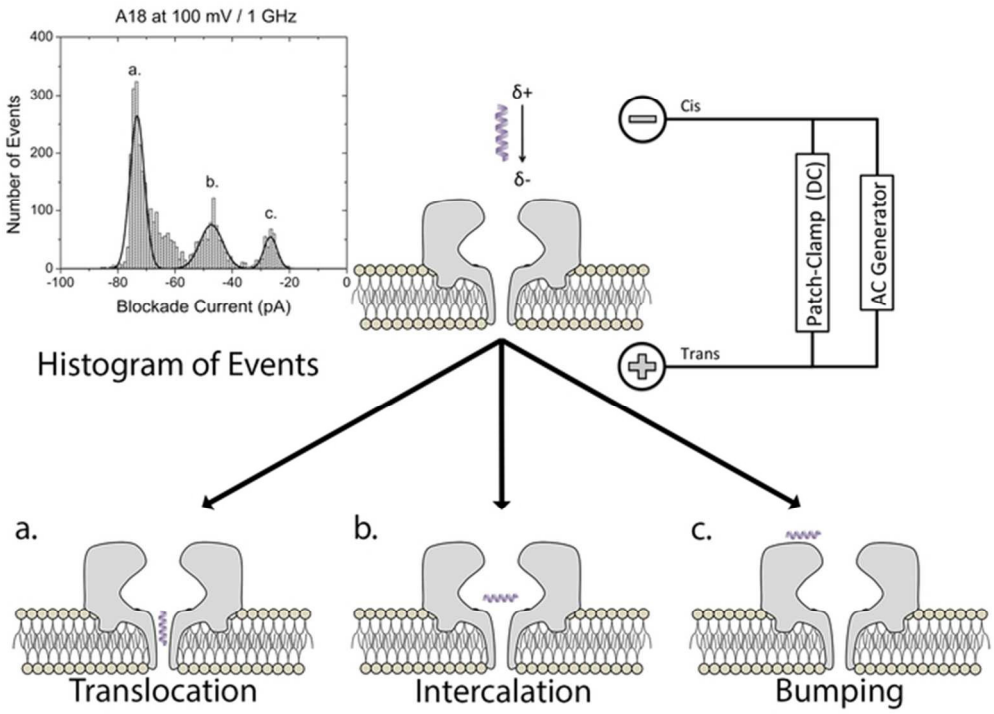

59x42mm (300 x 300 DPI)

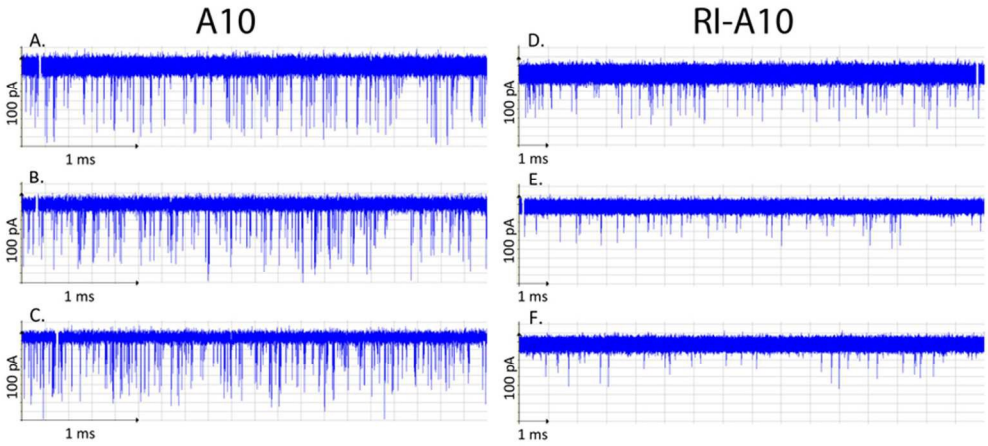

78x36mm (300 x 300 DPI)

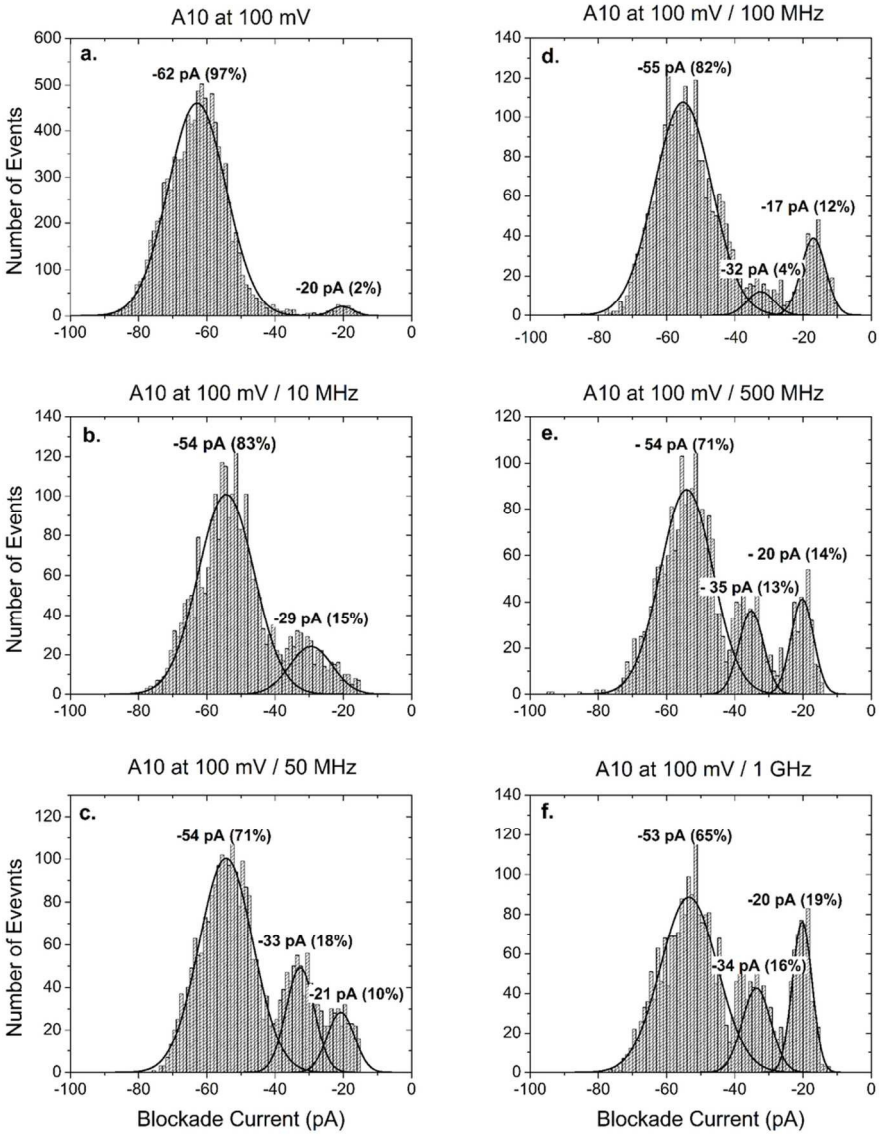

96x111mm (300 x 300 DPI)

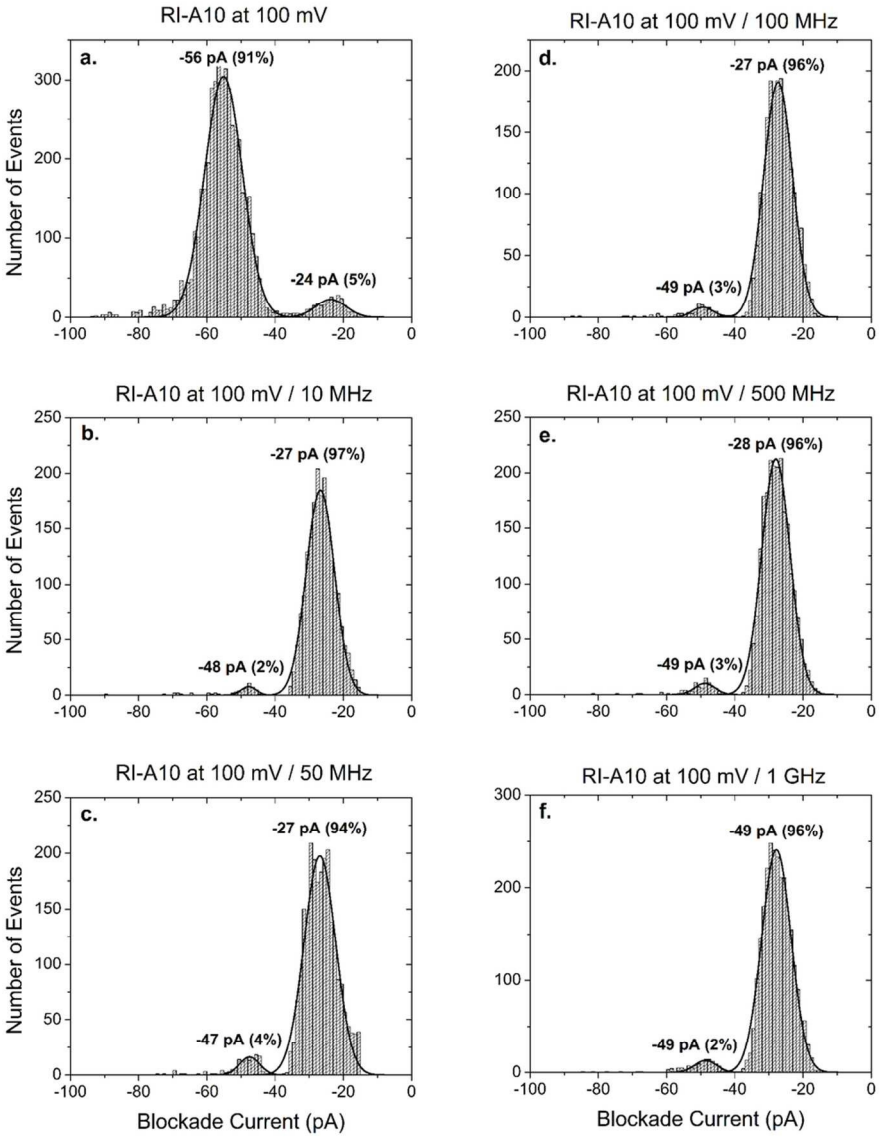

96x111mm (300 x 300 DPI)

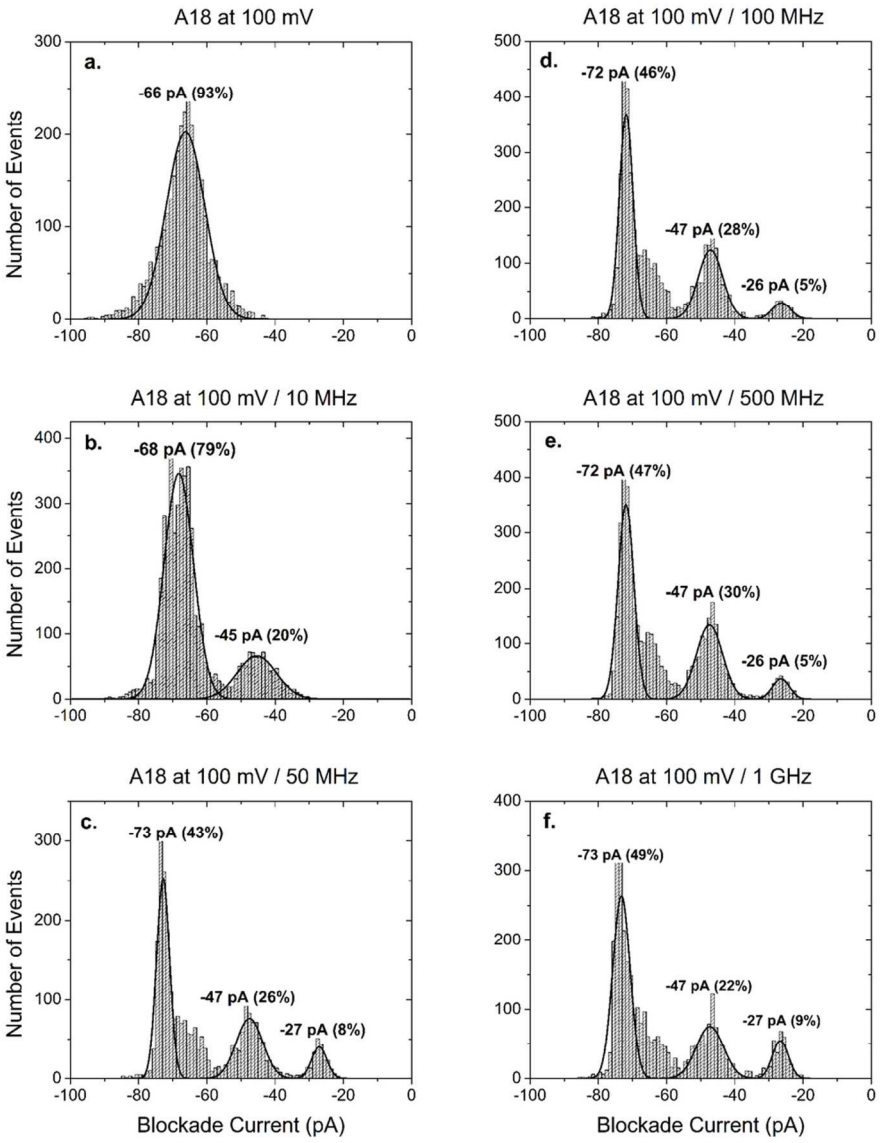

96x111mm (300 x 300 DPI)

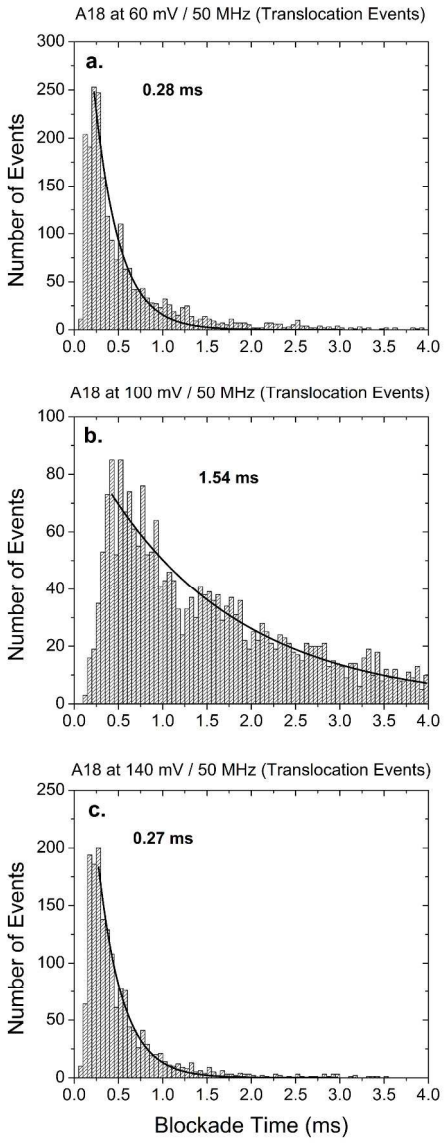

192x445mm (300 x 300 DPI)

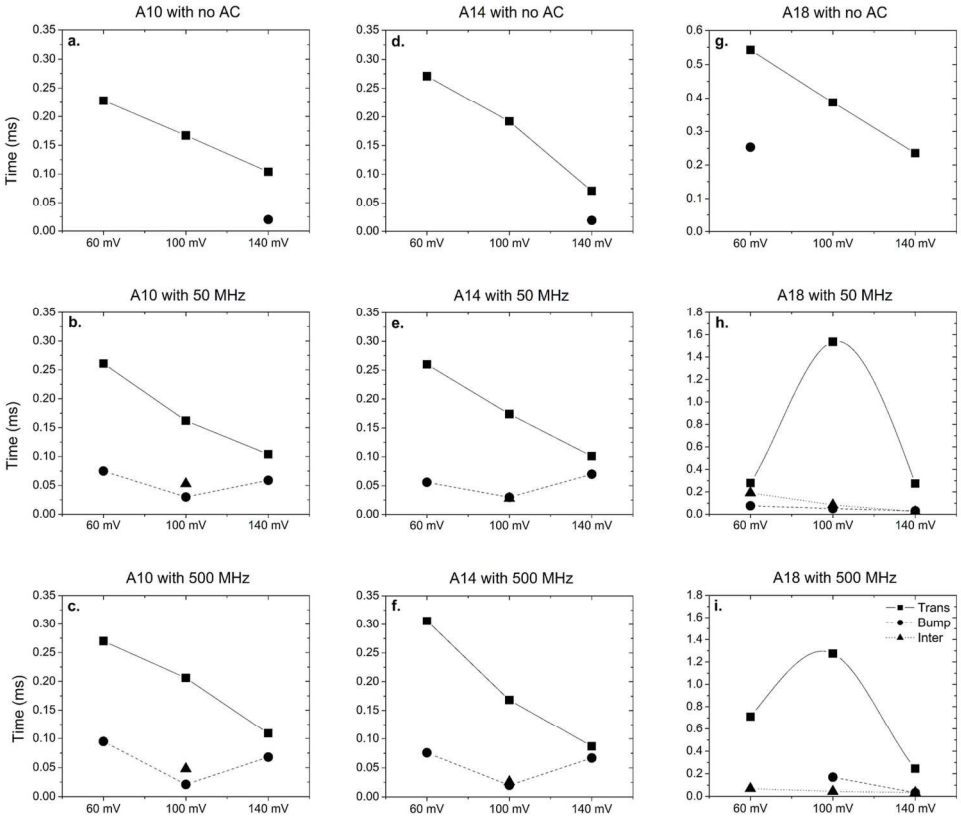

142x118mm (300 x 300 DPI)

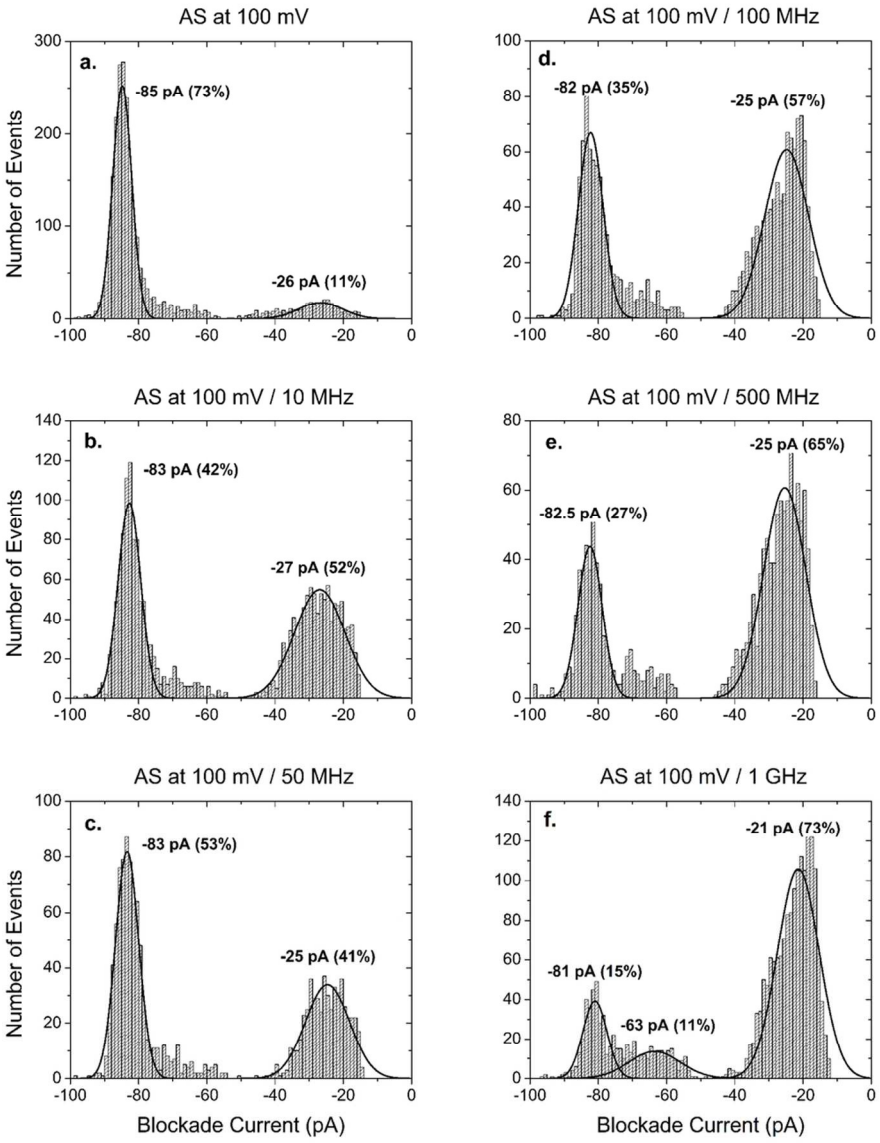

96x111mm (300 x 300 DPI)

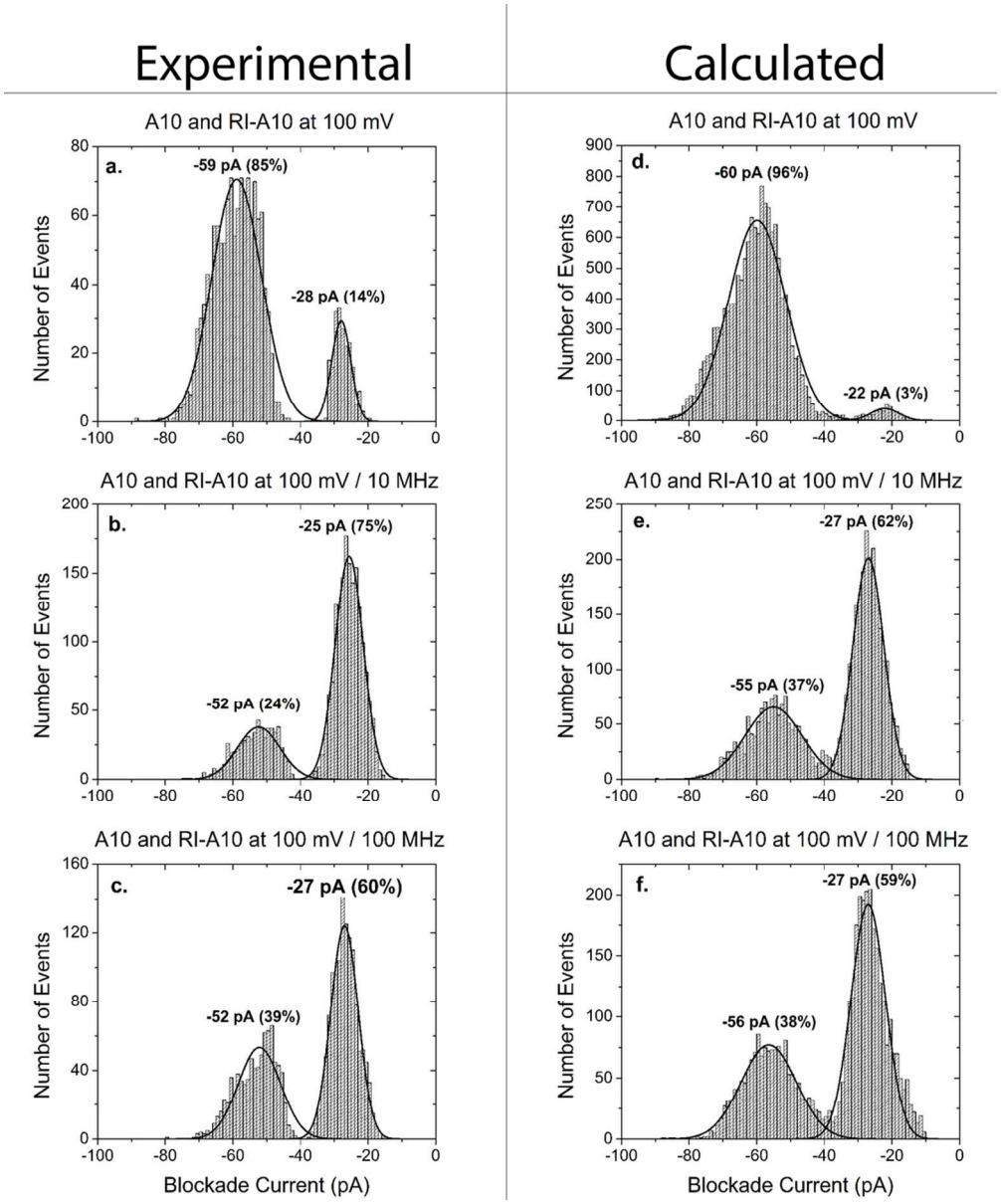

99x120mm (300 x 300 DPI)

There are three types of events when a peptide interacts with the pore. The AC field causes the peptide to oscillate at the entrance to the pore which can alter the type of event.